RSC Advances

ROYAL SOCIETY OF CHEMISTRY

www.rsc.org/advances

RSC Advances

ARTICLE

A new TICT and AIE-active tetraphenylethene-based Schiff base with reversible piezofluorochromism

Received 00th January 20xx,
Accepted 00th January 20xx

DOI: 10.1039/x0xx00000x

www.rsc.org/

Fangfang Han[a], Ran Zhang[a], Zhaoming Zhang[b], Jianguo Su[a] and Zhonghai Ni*[a]

A new tetraphenylethene-based Schiff base *N*-5-nitrosalicylidene-4-tetraphenylethenylamine (**NSTPE**) was synthesized based on 4-tetraphenylethenylamine and 5-nitrosalicylaldehyde, and its structure was fully characterized by ^{1}H NMR, ^{13}C NMR， MS and single crystal X-ray diffraction analysis. The study of optical properties shows that the emission exhibits interesting "on-off-on" switching property with a U-shaped tendency when adding water into the tetrahydrofuran solution of **NSTPE**, showing twisted intramolecular charge transfer (TICT) and aggregation-induced emission (AIE) characteristics. Moreover, the compound exhibits reversible piezofluorochromic properties.

1. Introduction

Organic photoactive functional materials have been paid everlasting attentions in the fields of chemistry, materials, physics, biology and life science due to their extensively practical and potential applications. Among the numerous organic photoactive materials, the optical switching materials under some outer stimulus such as light [1-5], electricity [6-12], magnetism [13], pressure [14-16], solvent [17-20], ion [21-24], molecule [25], pH value [26-27] and temperature [28-29] have aroused special interest. Generally, the optical switching of single molecule is relatively easy to realize in very dilute solution and several optical switching mechanisms have been proposed. However, the excellent optical switching materials of solid state are very limited because most of the luminogens are weakly emissive due to the well-known aggregation caused quenching (ACQ) [30-32]. In 2001, Tang's group found an opposite phenomenon that is the aggregation-induced emission (AIE) [33-38], which has become one of the mostly scientific hot topics very quickly. Up to date, several hundreds of AIE and aggregation-enhanced emission (AEE) [39-40] compounds have been synthesized and the corresponding possibly switching mechanisms also have been proposed.

Although many compounds show interesting AIE property, much effort has been paid on tetraphenylethene-based compounds because of not only their excellent AIE properties but also their facile synthesis and easy functionalization. Therefore, one of the most effective strategies for new AIE compounds is the design and synthesis of new tetraphenylethene-based compounds using tetraphenylethene as the starting precursor. Recently, we focus on the combination of tetraphenylethene unit with conventional Schiff base functional segment to develop new AIE compounds. Herein, we firstly report a new tetraphenylethene-based Schiff base **NSTPE** by the reaction of 4-tetraphenylethenylamine and 5-nitrosalicylaldehyde, which exhibits interesting "on-off-on" optical switching property due to the TICT [41] and AIE properties. To the best of our knowledge, the reports about "on-off-on" optical switching property are limited [42-43]. In addition, compound **NSTPE** exhibits reversible piezofluorochromic properties using two different optical samples recrystallized from CH_2Cl_2 and CH_3CH_2OH, respectively [44].

2. Experimental

2.1. Materials and instrumentation

In a nitrogen atmosphere, tetrahydrofuran (THF) and toluene (TOL) were distilled from sodium and benzophenone ketyl. Acetonitrile (MeCN) and dichloromethane (DCM) were distilled from calcium hydride. All other reagents and solvents were purchased commercially (AR grade) and used without further purification unless otherwise noted. The THF/H_2O mixtures with different water fractions were prepared by slowly adding distilled water into the THF solution of samples under ultrasound at room temperature. ^{1}H NMR and ^{13}C NMR spectra were collected on a Bruker-400 MHz spectrometer in DMSO solution with TMS as an internal standard. Mass spectra were obtained on a Bruker Ultraflextreme MALDI TOF/TOF mass spectrometer and a Jms-Q1000GC MK Ⅱ Ultra Quad GC/MS. UV-vis spectra were recorded on Shimadzu UV-3600 with a UV-VIS-NIR spectrophotometer. Emission spectra were performed by a HITACHI fluorescence spectrometer (F-4600). Crystal data of compound was selected on a Bruker APEX II CCDC diffractometer with graphite monochromated Mo-K radiation (λ = 0.71073 Å) at 298 K using the ω-scan technique. The structure was solved by direct methods with the SHELXS-97 computer program, and refined by full-matrix least-squares methods (SHELXL-97) on F^2. The ground state geometry of the molecule was fully optimized using density functional theory (DFT) at the B3LYP/6-31G (d, p) level, as implemented in Gaussian

*[a]School of Chemical Engineering and Technology, China University of Mining and Technology, Xuzhou 221116 Jiangsu Province, P. R. China. *E-mail: nizhonghai@cumt.edu.cn
[b]Institute for Catalysis, Hokkaido University, Sapporo, 001-0021, Japan
† Electronic Supplementary Information (ESI) available: CCDC number 1477929 (**NSTPE**). PL and NMR spectra.

09W [45] software package. Powder X-ray diffraction (PXRD) patterns were recorded on a Bruker D8 Advance X-ray diffractometer equipped with a Cu-Kα radiation (λ = 1.5418 Å, Cathode voltage = 40 kV and Cathode current = 30 mA).

2.2. Synthesis

2.2.1. Synthesis of 4-nitrotetraphenylethene (1)

Tetraphenylethene (TPE) (1.66 g, 5.0 mmol) was dissolved in ethyl acetate (70 mL). $Cu(NO_3)_2{\cdot}3H_2O$ (1.69 g. 7.0 mmol) and acetic anhydride (1.34 mL, 14.1 mmol) were added into the above solution. The mixture was stirred at 76 °C for 8 h, cooled to room temperature, and quenched with water. Then, the solution was extracted with DCM several times. The combined organic extracts were dried over $MgSO_4$, filtered, and concentrated under vacuum. The residue was purified by silica gel flash column chromatography using DCM/hexane (HEX) (1/6, v/v) as the eluent. Yield: 1.67 g, 89%. ^{1}H NMR (400 MHz, DMSO): δ 8.02 (2 H, d, *J* = 8.7 Hz), 7.23–7.12 (11 H, m), 7.00 (6 H, dt, *J* = 3.7, 2.1 Hz). ^{13}C NMR (101 MHz, DMSO): δ 151.04, 146.05, 142.94, 139.08–138.16, 132.39, 127.84, 123.55. GC/MSD: m/z 377 $[M]^+$.

2.2.2. Synthesis of 4-tetraphenylethenylamine (2)

Compound **1** (1.5 g, 4.0 mmol), 10% Pd/C (0.60 g) and hydrazine monohydrate (6.00 g, 120 mmol) were added in EtOH (80 mL). The mixture was refluxed for 4 h, then the solid Pd/C was filtered, and the solvent was removed under vacuum. Yield: 1.63 g, 96%. ^{1}H NMR (400 MHz, DMSO): δ 7.19–6.89 (17 H, m), 6.58 (2 H, d, *J* = 8.4 Hz), 6.28 (2 H, d, *J* = 8.4 Hz). ^{13}C NMR (101 MHz, DMSO): δ 147.77, 145.23–144.04, 141.65, 138.32, 132.42–130.48, 126.61, 113.57. GC/MSD: m/z 347 $[M]^+$.

2.2.3. Synthesis of *N*-5-nitrosalicylidene-4-tetraphenylethenylamine (NSTPE)

Compound **2** (0.34 g, 1.0 mmol) and 5-nitrosalicylaldehyde (0.17 g, 1.0 mmol) in ethanol (30 mL) were refluxed for 10 min, then a yellow solid was precipitated. The product was filtered and washed several times with ethanol and then collected with a high yield of 90%. ^{1}H NMR (400 MHz, DMSO): δ 14.42 (s, 1H), 9.14 (s, 1H), 8.64 (d, J = 2.9 Hz, 1H), 8.25 (dd, J = 9.2, 2.9 Hz, 1H), 7.29 (d, J = 8.5 Hz, 2H), 7.20–6.96 (m, 18H). ^{13}C NMR (101 MHz, DMSO): δ 167.46, 161.68, 144.69, 143.83–143.25, 141.62, 140.21, 139.52, 132.40, 131.64–130.99, 128.93, 128.76–128.20, 127.22, 121.48, 118.90. MALDI TOF-MS: m/z 496.313 $[M]^+$.

3. Results and discussion

3.1. Synthesis of NSTPE

The synthetic routes of the intermediates **1** and **2** and the target compound **NSTPE** are shown in Scheme 1 using TPE as the starting material. It is no doubt that the directional synthesis of intermediate 4-nitrotetraphenylethene is the key step for the preparation of the final product **NSTPE**. Herein, TPE is firstly nitrified by the mild nitrification system of $Cu(NO_3)_2{\cdot}3H_2O$ and acetic anhydride in ethyl acetate with high selectivity and yield. The intermediate **2** is synthesized simply by reduction reaction of **1** with hydrazine monohydrate using 10% Pd/C as a catalyst, which is one typical and common method for the reduction of nitro to amine group. Finally, the target TPE-based Schiff base is conveniently synthesized by the reaction of compound **2** with 5-nitrosalicylaldehyde with high yield. In a word, the intermediates **1** and **2** and the target compound are obtained with high yields and their synthetic methods are convenient and dependable.

3.2. Crystal structure of NSTPE

Yellow trip-like single crystals of **NSTPE** suitable for single crystal X-ray diffraction analysis were obtained by slow evaporation of DCM/methanol solution. The crystal data are given in Table 1 and the crystal structure of **NSTPE** is shown in Fig. 1. It is obvious that the **NSTPE** molecule is not planar. Instead, it adopts an asymmetrically twisted conformation and has a propeller-like structure. There is a relative larger planar paddle of Schiff base segment composed of 4-nitrophenol unit and a phenyl ring of TPE and their linking bridge C=N bond. The dihedral angle between the 4-nitrophenol unit and its linked phenyl ring of TPE is only 5.96°, which can be attributed to the existence of relatively strong intramolecular O–H---N hydrogen bond with the H---N distance of 1.780(4) Å. The bond length of C=N is 1.280(4) Å, and the length of C(3)–O(1) is 1.318(4) Å. The bond angle of C(1)–N(1)–C(8) is 122.28°. The packing diagrams of **NSTPE** are shown in Fig. 2. Though the 4-nitrophenol of two neighboring molecules are parallel to each other, the centroid distance of their benzene rings is 4.437(4)

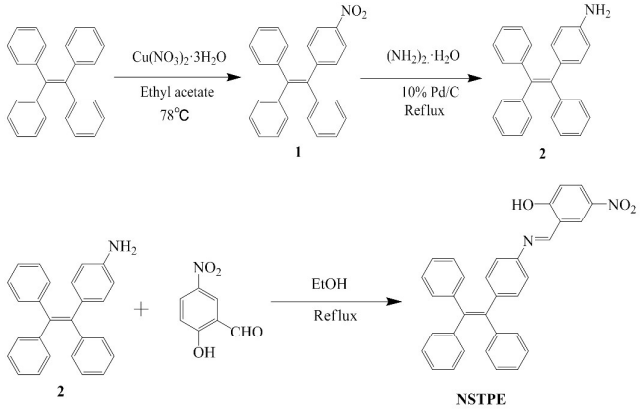

Scheme 1 Synthetic routes for **NSTPE**

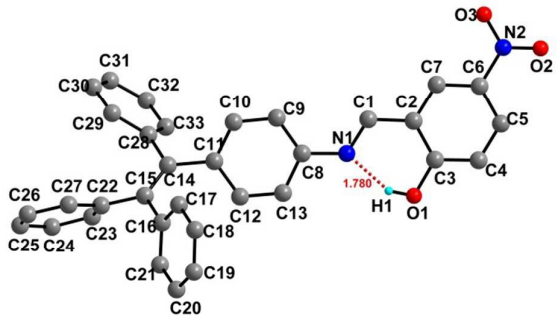

Fig. 1 Crystal structure diagram of compound **NSTPE**.

Table 1 Crystal data and structure refinement for single crystals of **NSTPE**

Empirical formula	$C_{33}H_{24}N_2O_3$	Z	2
Formula weight	496.54	$\rho_{Calcd.}$ (g cm^{-3})	1.263
Temperature (K)	296(2)	μ(Mo-$K\alpha$) (mm^{-1})	0.081
Crystal system	Triclinic	F(000)	520
Space group	P-1	Crystal size (mm)	0.12×0.06×0.02
a(Å)	5.616(3)	Measured reflections	1343
b(Å)	9.350(4)	Unique reflections [R_{int}]	1811[0.0445]
c(Å)	25.070(10)	Reflections (I > 2σ(I))	1811
α(°)	88.325(10)	GOF on F^2	1.000
β(°)	87.442(9)	R_1 [I > 2sigma(I)]	0.0599
γ(°)	83.160(9)	wR_2 (all data)	0.1165
Volume (Å^3)	1305.3(10)	ρ_{max} /ρ_{min}(e Å^{-3})	0.190/–0.166

Å (Fig. 2a), suggesting that the intermolecular π–π stacking interactions are very weak. In addition to the intramolecular hydrogen bonding, there also exist weak supramolecular C–H---O interactions. Firstly, two **NSTPE** units are connected together by C–H---O intermolecular hydrogen bonds (2.538(4) Å for C(4)–H(4)---O(1)) involving 4-nitrophenol benzene ring and hydroxyl oxygen atom, forming supramolecular dimeric structures. Then, these dimeric substructures are linked by C–H---O intermolecular interactions to form one-dimensional supramolecular chain-like structure in which the TPE units distribute at the two sides of the chain (Fig. 2b). These weak forces help the molecules to further rigidify their conformation and reduce the energy loss via the nonradiative relaxation channel.

3.3. Solvatochromic effect

The UV-vis absorption and photoluminescence (PL) spectra of compound **NSTPE** in HEX, TOL, CHL (chloroform), THF, DCM and MeCN are shown in Fig. 3a. The λ_{abs} appears at around 360 nm and shows an obviously blue-shift from 369 to 352 nm, which can be ascribed to the charge transfer from TPE unit to 4-nitrophenol segment. The intramolecular charge transfer [46-49] was further confirmed by their fluorescence spectra in solvents with varying polarity. The fluorescence images of the corresponding solutions are shown in Fig. 3b. Under UV light, NS**TPE** emits relatively strong green light in HEX, TOL and THF. However, it emits weak yellow light in CHL and DCM. The emission becomes nearly invisible in highly polar media such as MeCN. Evidently, the PL spectra indicate that the PL intensity quickly decreases accompanying an obvious red shift of λ_{em} from 522 to 551 nm with increasing the solvent polarity, which consists with the result in UV spectra (Fig. S1). The effects of solvents on the emissions can be further evaluated by the relationship between the solvent polarity parameter (Δf) and Stokes shift of the absorption and emission maxima (Lippert−Mataga equation) [50-51]. The detailed photophysical data are presented in Table 2. As show in Table 2, although the Δf of THF is higher than that of CHL, the emission wavelength of **NSTPE** in THF is shorter than that in CHL, which may be due to the interactions between the solute molecules and the solvent molecules. From the plots of $\Delta\upsilon$ versus Δf, we can find that the slope of the fitting line for **NSTPE** is as high as 6204.7**,** exhibiting significant solvatochromism effect (Fig. S3). This shows that the charge separation and dipole moment in the excited state is larger than in the ground state.

3.4. AIE and TICT properties

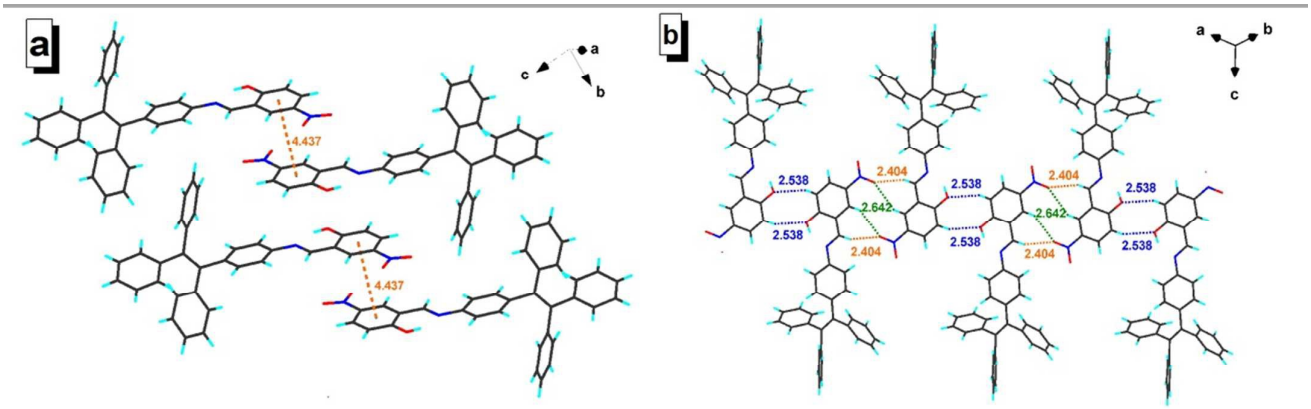

Fig. 2 Crystal packing diagrams of compound **NSTPE**.

Table 2 Optical transitions of **NSTPE** in different solvents[a].

Solvent	Δf	λ_{abs}	λ_{em}	Stokes shift
HEX	~0	369	522	7943.2
TOL	0.014	367	526	8236.5
CHL	0.149	366	545	8973.8
THF	0.210	363	525	8500.6
DCM	0.218	356	551	9941.1
MeCN	0.306	352	544	10026.7

[a] Abbreviations: Δf = orientational polarizability, λ_{abs} = lowest energy absorption maximum and λ_{em} = emission maximum.

The PL of **NSTPE** in THF and H_2O/THF has been measured to study its solvent polarity reduced emission and AIE property (Fig. 4). Compound **NSTPE** is highly soluble in THF and sparingly soluble in water. Different from the typical AIE compounds which are nearly no emission in pure THF solution, compound **NSTPE** emits obvious green light. With adding water into the THF solution of **NSTPE**, the emission intensity dramatically decreases. When the water content reaches to 10%, the emission is very weak accompanying significant red-shift, which is due to the increase of solvent polarity and the transformation from locally excited (LE) state to TICT state. Then, the emission keeps nearly "off" state until the content of water up to 65%. From 65% water content, the addition of water enhances the emission of **NSTPE**. Moreover, the emission is even stronger than its original THF solution when the water content is larger than 90%. In a word, with adding water into the THF solution of **NSTPE**, the emission exhibits interesting "on-off-on" switching property with a U-shaped tendency (Fig. S4). The extinction coefficients of **NSTPE** in different water content were listed in Table S1. Moreover, the fluorescence quantum yields of **NSTPE** in the H_2O/THF mixtures were measured, which displays the "on-off-on" switching property predictably (Table S1). To clearly elucidate the extraordinary phenomenon of **NSTPE** in H_2O/THF mixtures with different water fractions, quantum chemical optimization on their energy levels based on DFT/B3LYP/6-31G (d,

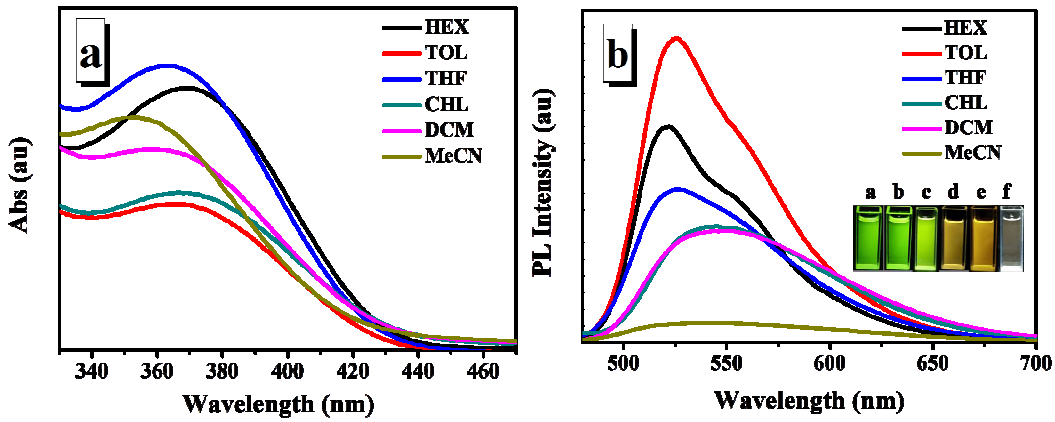

Fig. 3 (a) Absorption spectra of **NSTPE** in different organic solvents. (b) Emission spectra of **NSTPE** in different organic solvents. The insets emission images of NSTPE in HEX (a), TOL (b), THF (c),CHL (d), DCM (e) and MeCN (f) under 365 nm UV illumination with the concentration of 10^{-5} M and the excitation wavelength of 370 nm.

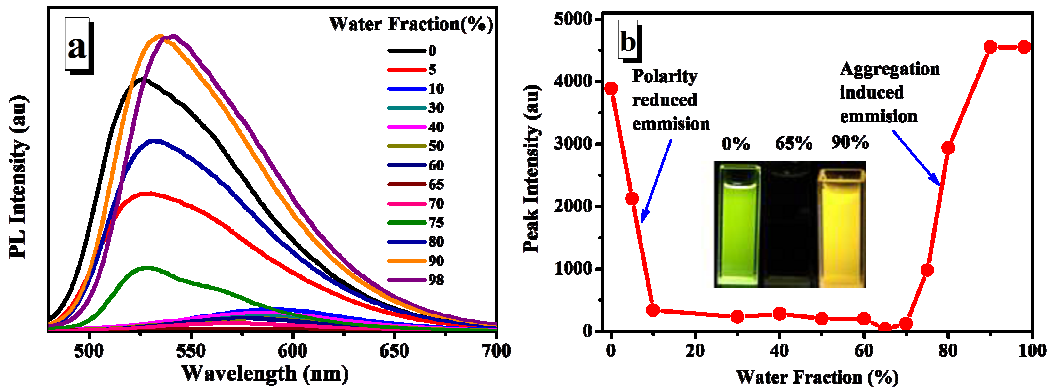

Fig. 4 (a) PL spectra of **NSTPE** in H_2O/THF mixtures with different water fractions. (b) Changes in PL peak intensity and emission images of the compound in different water fraction mixtures under 365 nm UV illumination with the concentration of 10^{-4} M and the excitation wavelength of 370 nm.

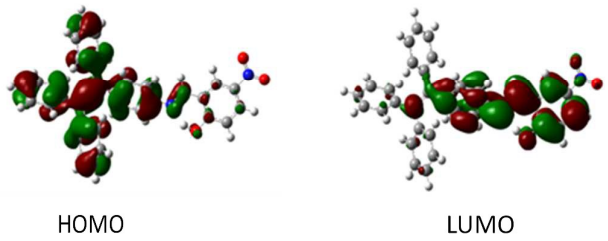

Fig. 5 Molecular orbital amplitude plots of the HOMO and LUMO of **NSTPE** calculated by using the B3LYP/6-31G basis set

p) using Gaussian09 was conducted. The highest occupied molecular orbital (HOMO) and lowest unoccupied molecular orbital (LUMO) diagrams of **NSTPE** are shown in Fig. 5. The HOMO of **NSTPE** is basically distributed over the TPE unit and the central C=N group, and the LUMO of **NSTPE** is mainly located at 4-nitrophenol unit and its neighboring one phenyl ring of TPE, which indicates that the **NSTPE** has an obvious tendency to form TICT state. According to the Franck–Condon principle, in the LE state, the molecule takes a planar conformation which is stabilized by the electronic conjugation in a nonpolar solvent. While in a polar solvent, intramolecular rotation brings the luminogen from the LE state to the TICT state, at which there is a total charge separation between D and A units. Then the twisted conformation is stabilized by the solvating effect of the polar solvent, which narrows the band gap and consequently red-shifts emission spectra (Fig. S1). TICT state is more likely to relax by nonradiative processes than by fluorescence emission in most cases, leading to the lower PL intensity in polar environments. But in aggregated state, intramolecular rotation is completely restricted and the molecule attains relatively planar aggregated geometry where energy loss due to TICT is hindered [52].

3.5. Piezofluorochromism

To further study the influence of aggregation morphology on emission, the recrystalliztion and grinding-fuming operations on compound **NSTPE** were carried out. Miraculously, there are two kinds emission for compound **NSTPE** when recrystallizing the

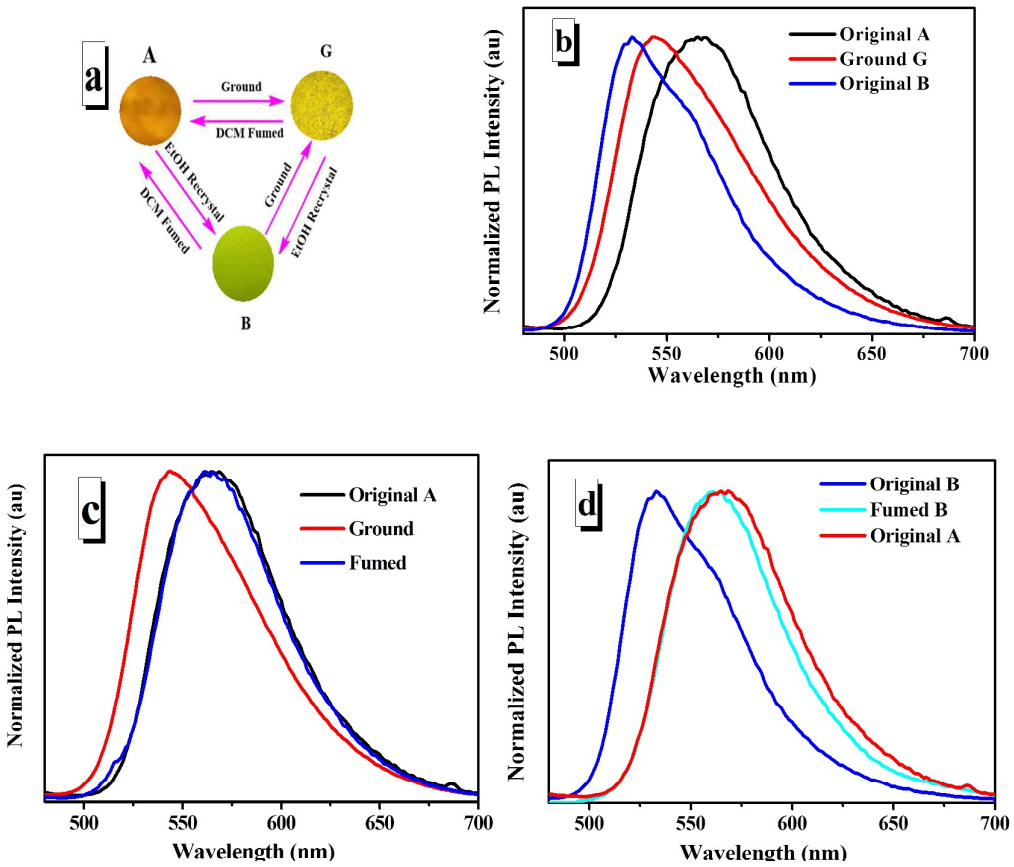

Fig. 6 (a) Fluorescence images of the powders: (A) **NSTPE** recrystal of DCM; (B) **NSTPE** recrystal of EtOH; (G) ground sample. (b) The normalized PL spectra of the three powders. (c) Change in the PL spectra of A by grinding–fuming process; (d) Change in the PL spectra of B by fuming process.

sample **NSTPE** of with DCM (A) and EtOH (B). Moreover, the two recrystallization samples exhibit reversible piezofluorochromic properties, in which the two crystal samples can transform to the same powder state G with bright yellow emission. Finally, the transformation of the three kinds of emission forms a reversible circle under the recrystalliztion and grinding-fuming operations as shown in Fig. 6a. The detailed emission and reversible emission transformation among the three kinds of samples are shown in Fig. 6b-d and Fig. S1. The crystal A of **NSTPE** exhibits a stronger orange-light emission centered at 572 nm, whereas its crystal B shows yellowish green emission centered at 532 nm. Upon grinding using a spatula or a pestle, both of the emissions of A and B become faint yellow G with the emission peak at around 543 nm. The emission color of the ground sample G can be entirely restored to orange A upon fuming with solvent DCM (Fig. 6c) and it also can be transformed to B by recrystallizing with EtOH (Fig. S2), which suggests that the piezochromic fluorescence process is reversible. Moreover, when crystal B is exposed to solvent DCM, the PL spectrum of B also changes remarkably, passing from an initial yellowish green yellow to orange light of A (Fig. 6d).

To confirm the relationship between aggregation morphology and emission wavelength, compound **NSTPE** at different aggregated states were analyzed by powder X-ray diffraction (PXRD). The PXRD diffractograms of A and B exhibit many sharp diffraction peaks, indicating their crystalline nature (Fig. 7). After grinding, the disappearance of most diffraction peaks indicates a significant change from the self-assembled crystalline architecture to amorphous state. When the faint yellow powders (G) are fumed with solvent vapor, sharp diffraction peaks emerge again, suggesting that the transformation from amorphous state to crystalline state of **NSTPE**.

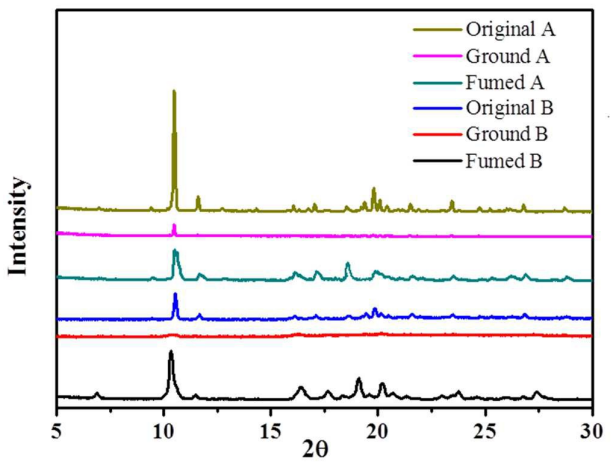

Fig. 7 PXRD patterns of **NSTPE** in different morphologies.

4. Conclusion

In summary, a new TPE-based Schiff base **NSTPE** with D-A structure has been designed and synthesized. Interestingly, compound **NSTPE** exhibits two different TICT and AIE photoresponsive properties. With adding water into the THF solution of **NSTPE**, the emission exhibits interesting "on-off-on" switching property with a U-shaped tendency. Multiple different reversible emissions have been observed under the operations of grinding-fuming and recrystallization on **NSTPE** with different solvents, which can be attributed to the reversible changes of different morphology states. This work further confirms that using TPE as the precursor is one of the most effective strategies to construct AIE compounds especially for multifunctional materials.

Acknowledgements

This work was supported by the Fundamental Research Funds for the Central Universities (2015XKZD08) and the Priority Academic Program Development of Jiangsu Higher Education Institutions.

References

1 H. B. Chen, and Y. Liao, *J. Photoch. Photobio. A*, 2015, **300**, 2226.
2 J. Han, Y. Zang, Z. Yu, Y. He and P. Guo, *Tetrahedron Lett.,* 2015, **56**, 5213–5217.
3 D. A. Safin, M. Bolte and Y. Garcia, *CrystEngComm.,* 2014, **16**, 8786–8793.
4 X. D. Yang, C. Chen, Y. J. Zhang, L. X. Cai and J. Zhang, *Inorg. Chem. Commun.,* 2015, **60**, 122–125.
5 Y. Yonezaki and S. Takei, *J .Lumin.,* 2015, **173**, 237–242.
6 W. J. Li, D. D. Liu, F. Z. Shen, D. Ma, Z. M. Wang, T. Feng, Y. X. Xu, B. Yang and Y. G. Ma, *Adv. Funct. Mater.,* 2012, **22**, 2797–2803.
7 Y. Liu, S. M. Chen, J. W. Y. Lam, P. Lu, R. T. K. Kwok, F. Mahtab, H. S. Kwok and B. Z. Tang, *Chem. Mater.,* 2011, **23**, 2536–2544.
8 U. Mitschke and P. Bäuerle, *J. Mater. Chem.,* 2000, **10**, 1471–1507.
9 R. Zhang, Y. Zhao, G. L. Li, D. S. Yang and Z. H. Ni, *RSC Adv.,* 2016, **6**, 9037–9048.
10 X. J. Zhang, A. S. Shetty and S. A. Jenekhe, *Macromolecules,* 1999, **32**, 7422–7429.
11 R. Zhang, Y. Zhao, T. F. Zhang, L. Xu and Z. H. Ni, *Dyes Pigments,* 2016, **130**, 106–115.
12 M. A. Kostiainen, P. Ceci, M. Fornara, P. Hiekkataipale, O. Kasyutich, R. J. M. Nolte, J. J. L. M. Cornelissen, R. D. Desautels and J. Lierop, *Nano.*, 2011, **5**, 6394–6402.
13 Z. G. Chi, X. Q. Zhang, B. J. Xu, X. Zhou, C. P. Ma, Y. Zhang, S. W. Liu and J. R. Xu, *Chem. Soc. Rev.*, 2012, **41**, 3878–3896.
14 R. Misra, T. Jadhav, B. Dhokale and S. M. Mobin, *Chem. Commun.*, 2014, **50**, 9076–9078.
15 X. Q. Zhang, Z. G. Chi, B. J. Xu, C. J. Chen, X. Zhou, Y. Zhang, S. W. Liu and J. R. Xu, *J. Mater. Chem.,* 2012, **22**, 18505–18513.
16 M. P. Aldred, G. F. Zhang, C. Li, G. Chen, T. Chen and M. Q. Zhu, *J. Mater. Chem. C,* 2013, **1**, 6709–6718.
17 T. Jadhav, B. Dhokale and R. Misra, *J. Mater. Chem. C,* 2015, **3**, 9063–9068.
18 C, Liu, W. He, G. Shi, H. Y. Luo, S. Zhang and Z. G. Chi, *Dyes Pigments,* 2015, **112**, 154–161.
19 C. X. Niu, Y. You, L. Zhao, D. C. He, N. Na and J. Ouyang, *Chemistry,* 2015, **21**, 13983–13990.
20 M. H. Lee, H. Lee, M. J. Chang, H. S. Kim, C. Kang and J. S. Kim, *Dyes Pigments,* 2016, **130**, 245–250.
21 J. L. Tang, C. Y. Li, Y. F. Li, X. Lu and H. R. Qi, *Anal. Chim.*

Acta., 2015, **888**, 155–161.
22 X. R. Wang, J. M. Hu, T. Liu, G. Y. Zhang and S. Y. Liu, *J. Mater. Chem.,* 2012, **22**, 8622–8628.
23 Y. Wang, Y. W. Liu, J. F. Miao, M. H. Ren, W. Guo and X. Lv, *Sensor. Actuat. B-Chem.,* 2016, **226**, 364–369.
24 Y. B. Cai, L. Z. Li, Z. T. Wang, J. Z. Sun, A. J. Qin and B. Z. Tang, *Chem. Commun.*, 2014, **50**, 8892–8895.
25 C. P. Ma, B. J. Xu, G. Y. Xie, J. J. He, X. Zhou, B. Y. Peng, L. Jiang, B. Xu, W. J. Tian, Z. G. Chi, S. W. Liu, Y. Zhang and J. R. Xu, *Chem. Commun.*, 2014, **50**, 7374–7377.
26 T. Y. Han, X. Feng, D. D. Chen and Y. P. Dong, *J. Mater. Chem. C*, 2015, **3**, 7446–7454.
27 Y. W. Ma, Y. Li, L. G. Chen, Y. Xiong and G. H. Yin, *Dyes Pigments*, 2016, **126**, 194–201.
28 W. Oh, S. Angupillai, P. Muthukumar, H. S. So and Y. Son, *Dyes Pigments*, 2016, **128**, 235–245.
29 J. Z. Liu, J. W. Y. Lam and B. Z. Tang, *Chem. Rev.*, 2009, **109**, 5799–5867.
30 T. P. I. Saragi, T. Spehr, A. Siebert, L. T. Fuhrmann and J. Salbeck, *Chem. Rev.*, 2007, **107**, 1011–1065.
31 A. C. Grimsdale, K. L. Chan, R. E. Martin, P. G. Jokisz and A. B. Holmes, *Chem. Rev.*, 2009, **109**, 897–1091.
32 Z. M. Zhang, Y. Zhao, R. Zhang, L. F. Zhang, W. Q. Cheng and Z. H. Ni, *Dyes Pigments*, 2015, **118**, 95–101.
33 J. D. Luo, Z. L. Xie, J. W. Y. Lam, L. Cheng, B. Z. Tang, H.Y. Chen, C. F. Qiu, H. S. Kwok, X. W. Zhan, Y. Q. Liu and D. B. Zhu, *Chem. Commun.*, 2001, 1740–1741.
34 Z. Li, Y. Q. Dong, B. X. Mi, Y. H. Tang, M. Häussler, H. Tong, Y. P. Dong, J. W. Y. Lam, Y. Ren, H. H. Y. Sung, K. S. Wong, P. Gao, I. D. Williams, S. K. Hoi and B. Z. Tang, *J. Phys. Chem. B*, 2005, **109**, 10061–10066.
35 G. Yu, S. W. Yin, Y. Q. Liu, J. S. Chen, X. J. Xu, X. B. Sun, D. Ma, X. W. Zhan, Q. Peng, Z. G Shuai, B. Z. Tang, D. B. Zhu, W. H. Fang and Y. Luo, *J. Am. Chem. Soc.*, 2005, **127**, 6335–6346.
36 Z. M. Zhang, F. F. Han, R. Zhang, N. Li and Z. H. Ni, *Tetrahedron Lett.*, 2016, **57**, 1917–1920.
37 J. Mei, N. L. C. Leung, R. T. K. Kwok, J. W. Y. Lam and B. Z. Tang, *Chem. Rev.*, 2015; 115: 11718–940.
38 J. Mei, Y. Hong, J. W. Y. Lam, A, Qin, Y. Tang and B. Z. Tang, *Adv. Mater.*, 2014; 26:5429–79.
39 B. K. An, S. K. Kwon, S. D. Jung and S. Y. Park, *J. Am. Chem. Soc.*, 2002, **124**, 14410–14415.
40 X. Q. Zhang, Z. G. Chi, X. Zhou, S. W. Liu, Y. Zhang and J. R. Xu, *J .Phys. Chem. C*, 2012, **116**, 23629–23638.
41 E. Lager, J. Z. Liu, A. Aguilar-Aguilar, B. Z. Tang and C. E. Peña, *J. Org. Chem.*, 2009, **74**, 2053–2058.
42 D. Ding, K. Li, B. Liu and B. Z. Tang, *Acc. Chem. Res.*, 2012, **46**, 2441–2453.
43 Z. L. Xie, C. J. Chen, S. D. Xu, J. Li, Y. Zhang, S. W. Liu, J. R. Xu and Z. G. Chi, *Angew. Chem. Int. Ed.*, 2015, **54**, 7181–7184
44 N. Zhao, Z. Y. Yang, J. W. Lam, H. H. Y. Sung, N. Xie, S. J. Chen, H. M. Su, M. Gao, I. D. Williams, K. S. Wong, B. Z. Tang, *Chem. Commun.*, 2012, **48**, 8637–8639.
45 K. R. Wee, H. C. Ahn, H. J. Son, W. S. Han, J. E. Kim, D. W. Cho and S. O. Kang, *J. Org. Chem.*, 2009, **74**, 8472–8475.
46 E. Ragnoni, D. M. Di, A. Iagatti, A. Lapini and R. Righini, *J. Phys. Chem. B*, 2015, **119**, 420–432.
47 Y. J. Zhang, K. Wang, G. L. Zhuang, Z. Q. Xie, C. Zhang, F. Cao, G. X. Pan, H. F. Chen, B. Zou and Y. G. Ma, *Chemistry*, 2015, **21**, 2474–2479.
48 S. I. Druzhinin, V. A. Galievsky, A. Demeter, S. A. Kovalenko, T. Senyushkina, S. R. Dubbaka, P. Knochel, P. Mayer, C. Grosse, D. Stalke and K. A. Zachariasse, *J. Phys. Chem. A*, 2015, **119**, 11820–11836.
49 V. A. Galievsky, S. I. Druzhinin, A. Demeter, P. Mayer, S. A. Kovalenko, T. A. Senyushkina, K. A. Zachariasse, *J. Phys. Chem. A*, 2010, **114**, 12622–12638.
50 E. Z. Lippert, *Naturforsh., A: Phys. Sci.*, 1955, **10**, 541−545.
51 N. Mataga, Y. Kaifu and M. Koizumi, *Bull. Chem. Soc. Jpn.,* 1956, **29**, 465−470.
52 R. R. Hu, E. Lager, A. Aguilar-Aguilar, J. Z. Liu, J. W. Y. Lam, H. H. Y. Sung, I. D. Williams, Y. C. Zhong, K. S. Wong, C. E. Peña and B. Z. Tang, *J. Phys. Chem. C*, 2009, **113**, 15845–15853.

A new TICT and AIE-active tetraphenylethene-based Schiff base with reversible piezofluorochromism

Fangfang Han, Ran Zhang, Zhaoming Zhang, Jianguo Su, Zhonghai Ni*

Synopsis

A new tetraphenylethene-based Schiff base *N*-5-nitrosalicylidene-4-tetraphenylethenylamine (**NSTPE**) exhibits interesting "on-off-on" optical switching property and reversible piezofluorochromic properties using two different optical samples recrystallized from CH_2Cl_2 and CH_3CH_2OH, respectively.